Evidence of a universal scaling relationship for leaf CO_2 drawdown along an aridity gradient

I. Colin Prentice[1,2,3], Tingting Meng[3], Han Wang[1,3], Sandy P. Harrison[1,3,4], Jian Ni[3,5] and Guohong Wang[3]

[1]Department of Biological Sciences, Macquarie University, North Ryde, NSW 2109, Australia; [2]Grantham Institute and Division of Biology, Imperial College, Silwood Park, Ascot SL5 7PY, UK; [3]State Key Laboratory of Vegetation and Environmental Change, Institute of Botany, Chinese Academy of Sciences, Xiangshan Nanxincun 20, 100093 Beijing, China; [4]School of Geographical Sciences, University of Bristol, Bristol BS8 1SS, UK; [5]Alfred Wegener Institute for Polar and Marine Research, Telegrafenberg A43, D-14473 Potsdam, Germany

Summary

Author for correspondence:
I. Colin Prentice
Tel: +61 2 9850 4227
Email: colin.prentice@mq.edu.au

- The leaf carbon isotope ratio ($\delta^{13}C$) of C_3 plants is inversely related to the drawdown of CO_2 concentration during photosynthesis, which increases towards drier environments. We aimed to discriminate between the hypothesis of universal scaling, which predicts between-species responses of $\delta^{13}C$ to aridity similar to within-species responses, and biotic homoeostasis, which predicts offsets in the $\delta^{13}C$ of species occupying adjacent ranges.
- The Northeast China Transect spans 130–900 mm annual precipitation within a narrow latitude and temperature range. Leaves of 171 species were sampled at 33 sites along the transect (18 at $\geq$ 5 sites) for dry matter, carbon (C) and nitrogen (N) content, specific leaf area (SLA) and $\delta^{13}C$.
- The $\delta^{13}C$ of species generally followed a common relationship with the climatic moisture index (MI). Offsets between adjacent species were not observed. Trees and forbs diverged slightly at high MI. In C_3 plants, $\delta^{13}C$ predicted N per unit leaf area (N_{area}) better than MI. The $\delta^{13}C$ of C_4 plants was invariant with MI. SLA declined and N_{area} increased towards low MI in both C_3 and C_4 plants.
- The data are consistent with optimal stomatal regulation with respect to atmospheric dryness. They provide evidence for universal scaling of CO_2 drawdown with aridity in C_3 plants.

Introduction

Stable carbon isotope ratios ($\delta^{13}C$ values) measured on the leaves of C_3 plants are linearly and inversely related to the time-averaged drawdown of CO_2 concentration during photosynthesis (Farquhar *et al.*, 1982). Many studies of foliar $\delta^{13}C$ in C_3 plants have reported a trend towards higher (less negative) values at drier sites (e.g. Stewart *et al.*, 1995; Miller *et al.*, 2001; Midgley *et al.*, 2004; Liu *et al.*, 2005; Wittmer *et al.*, 2008). This relationship also applies globally, and dominates relationships of $\delta^{13}C$ with all other geographic and climatic variables (Diefendorf *et al.*, 2010). One study showed a similar scaling of the $\delta^{13}C$ of respired CO_2 with moisture availability both within and between communities dominated by four tree species (Bowling *et al.*, 2002). However, a few studies of leaf $\delta^{13}C$ along moisture gradients have yielded results that are harder to interpret (e.g. Schulze *et al.*, 1996, 2006). Schulze *et al.*

(1998, 2006) proposed the hypothesis that within-species responses of $\delta^{13}C$ are steeper than the overall community-level response, implying a homeostatic role for beta diversity in maintaining photosynthetic rates. No published evidence unambiguously supports this hypothesis. However, its opposite, that is, universal scaling (with similar responses shown by species and communities), is not strongly supported either, because very few studies have sampled individual species repeatedly along aridity gradients.

Experiments have shown that stomatal conductance (g_s) responds to transpiration rate (Mott & Parkhurst, 1991; Pieruschka *et al.*, 2010). This is indistinguishable in the field from a response to vapour pressure deficit (D). D is an atmospheric property shared by the plants in a community, controlled in part by transpiration itself (Monteith, 1995). Conditions where transpiration is restricted because of low soil water availability typically co-occur with high values of D. The ratio of internal to ambient CO_2 concentration

$(c_i : c_a)$ is related to g_s through the diffusion equation, $A = g_s c_a (1 − c_i : c_a)$, where g_s is the stomatal conductance to CO_2 and A is the net assimilation rate. The optimality hypothesis of Cowan & Farquhar (1977) predicts a dependence of the form $c_i : c_a = 1/(1 + \xi\sqrt{D})$ or, with a further approximation, $c_i : c_a = 1 − \xi\sqrt{D}$ (the two equations are close within the commonly encountered ranges of $c_i : c_a$ and D), where ξ is related to Cowan and Farquhar's λ parameter which represents an 'exchange rate' between carbon and water. This prediction can readily be derived for an assumed linear relationship between A and c_i, but it has recently been shown to remain a good approximation under more realistic assumptions (Katul *et al.*, 2010; B. Medlyn, pers. comm.). It is theoretically expected that ξ will increase with soil moisture deficit, leading to a steeper relation of $c_i : c_a$ to D along soil moisture gradients than would be predicted for constant ξ. This expectation is supported by direct measurements of the g_s–D relationship in different species and environments (e.g. Palmroth *et al.*, 1999; B. Medlyn, pers. comm.). In principle, ξ could also vary among species and plant functional types. However, very little empirical information is available to indicate whether such differences exist, or whether adjustment in ξ along aridity gradients occurs mainly within species, occurs mainly between species, or is universal (i.e. following the same relationship within and between species).

Although D is highly variable in time, we would expect that $\delta^{13}C$ measurements would relate to time-averaged values of D and, most importantly, that these values of D would be similar for all plants at a site (except in dense vegetation where subcanopy species experience reduced D). Thus, leaf $\delta^{13}C$ measured on all species in a community should provide evidence for or against a universal scaling of $c_i : c_a$ with D. Differences among species or plant functional types might be attributed to differences in ξ related, for example, to differences in conducting tissue properties or rooting strategy.

We set out to test the hypothesis of universal scaling by analysing leaf samples of the most common vascular plant species at 33 sites distributed along the Northeast China Transect (NECT; Fig. 1). The NECT runs east–west (so there is no confounding with latitude) with little variation in mean annual temperature (0–6°C), but a major variation in annual precipitation from 130 to 900 mm. There is a steady trend of decreasing stature, density and foliage projective cover towards the dry end of the transect, with trees largely confined to the wet end (Ni & Zhang, 2000; Ni & Wang, 2004; Wang & Ni, 2005). Thus, the NECT has ideal properties for an aridity gradient study. In order to examine other correlates of leaf $\delta^{13}C$ we measured leaf dry matter, carbon (C) and nitrogen (N) contents and specific leaf area (SLA), allowing us to evaluate ancillary findings in the literature that relate to the potential trade-off between leaf N and stomatal closure. Sampling density was sufficient that many species were sampled at more than one site. Altogether 18 species, distributed fairly evenly along the gradient, were sampled at five or more sites, allowing us to analyse the within-species patterns and to compare these with the multi-species trends.

Materials and Methods

Environmental data

Mean monthly values of temperature, precipitation and percentage of possible sunshine hours were derived from 1814 meteorological stations across China (740 stations have observations from 1971–2000, and the rest from 1981–1990: China Meteorological Administration, unpublished data). The climate data were interpolated at 1-km resolution using a smoothing spline interpolation (ANUSPLIN version 4.36; Hutchinson & Hancock, 2006) and the STRM 1-km digital elevation model (Farr *et al.*, 2007). Mean annual temperature (MAT), mean annual precipitation
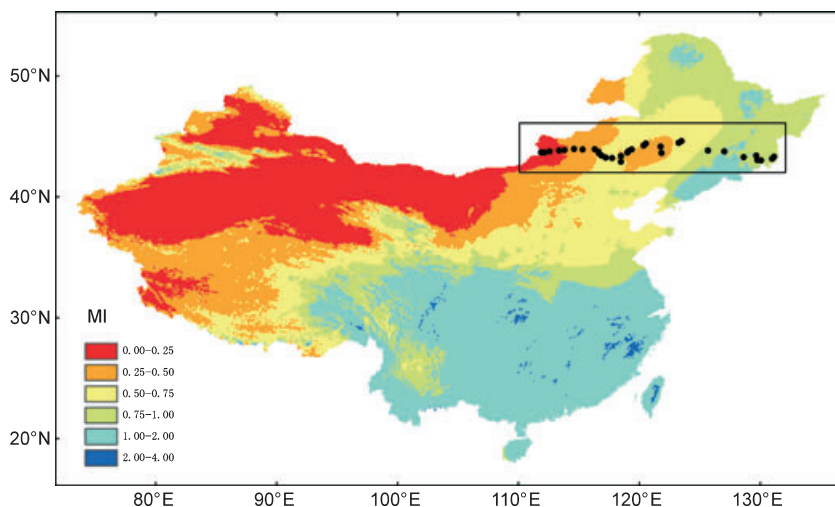

Fig. 1 Location of the Northeast China Transect (NECT; rectangle) in China. Sites are shown as closed black circles. Gradients in the climatic moisture index (MI) are indicated by colour fields.

(MAP), and mean precipitation in June, July and August (PJJA) were calculated for each site. Bioclimatic variables more closely related to the physiological controls on plant growth were then derived as in Prentice *et al.* (1993) and Gallego-Sala *et al.* (2010): the mean temperature of the coldest month (MTCO), the daily mean during the growing season (the period with daily-interpolated temperatures > 0°C) of accumulated growing degree days above 0°C (mGDD$_0$, equivalent to growing-season mean temperature), the daily mean during the growing season of photosynthetically active radiation (mPAR$_0$), annual equilibrium evapotranspiration (EET), the climatic moisture index (MI = MAP/EET), annual actual evapotranspiration (AET) and the alpha index (alpha = AET/EET). The last two variables require data on available water holding capacity (AWHC). Texture data (sand, silt and clay fractions) were obtained for soil types, digitized from the 1 : 1 million soil map of China (Shi *et al.*, 2004). AWHC was then calculated as the difference between field capacity and wilting point, estimated as the soil water content at matric

potentials of −0.033 and −1.5 MPa, respectively, using the equations of Saxton & Rawls (2006) with a correction (based on linear interpolation of the cumulative log size–frequency plot) to convert from International Society for Soil Sciences (ISSS) to US Department of Agriculture (USDA) definitions of the sand–silt boundary.

Sampling strategy

The sampling sites (Table 1) were selected to represent the aridity gradient along the transect. All sampling took place during August 2006. All sites were occupied by visually homogeneous uncultivated vegetation. Most of the grasslands are grazed, and it is virtually impossible to find undisturbed sites; we chose sites with minimal signs of recent disturbance, and avoided sites with evidence of exceptionally high grazing pressure.

Species composition and vegetation structure were surveyed at each site. In each of the eight forested sites at the eastern (wet) end of the transect, we surveyed one 10 ×

Table 1 Characteristics of the sites from the Northeast China Transect (NECT) used in this analysis

Site no.	Longitude (degree)	Latitude (degree)	Elevation (m)	Vegetation types	Max height (m)	No. of species sampled	Moisture index (MI) at the site
NECT01	118.48	42.88	1024	Steppe	0.36	7	0.50
NECT02	119.02	43.64	781	Steppe	0.58	13	0.50
NECT03	129.78	43.02	136	Mixed deciduous broad-leaved forest	10.5	17	0.77
NECT04	130.08	42.98	114	Mixed deciduous broad-leaved forest	7.5	15	0.78
NECT05	131.15	43.30	289	Mixed conifer–deciduous broad-leaved forest	17.5	25	0.79
NECT06	131.00	43.12	244	Mixed deciduous broad-leaved forest	26.0	20	0.78
NECT07	129.67	43.39	224	Mixed conifer–deciduous broad-leaved forest	19.0	15	0.82
NECT08	128.64	43.25	601	Conifer forest	23.5	13	0.96
NECT09	127.03	43.73	390	Mixed deciduous broad–leaved forest	23.0	19	0.95
NECT10	125.68	43.81	252	Mixed conifer–deciduous broad–leaved forest	6.0	14	0.79
NECT11	123.51	44.59	146	Meadow steppe	0.75	11	0.55
NECT12	123.27	44.43	150	Meadow steppe	0.20	7	0.51
NECT13	121.84	43.60	203	Meadow steppe	0.53	10	0.44
NECT14	121.77	44.12	202	Meadow steppe	0.36	5	0.43
NECT15	120.55	44.39	448	Steppe	0.90	11	0.51
NECT16	120.37	44.22	372	Steppe	0.53	12	0.45
NECT17	119.38	43.88	601	Steppe	0.57	12	0.48
NECT18	119.12	43.76	729	Steppe	0.76	12	0.47
NECT19	118.49	43.34	707	Steppe	0.43	5	0.47
NECT20	117.76	43.19	889	Steppe	0.75	11	0.48
NECT21	117.24	43.22	1259	Steppe	1.30	13	0.57
NECT22	116.89	43.39	1267	Steppe	0.42	7	0.55
NECT23	116.68	43.55	1261	Steppe	0.70	13	0.51
NECT24	116.64	43.69	1211	Steppe	0.58	10	0.49
NECT25	116.31	43.91	1199	Steppe	0.90	12	0.46
NECT26	115.32	43.90	1196	Steppe	0.65	13	0.38
NECT27	114.61	43.94	1123	Desert steppe	0.60	9	0.30
NECT28	113.83	43.83	1166	Desert steppe	0.23	8	0.27
NECT29	113.36	43.80	1017	Desert steppe	0.28	6	0.22
NECT30	112.59	43.72	974	Desert steppe	0.30	9	0.18
NECT31	112.17	43.63	999	Desert steppe	0.24	8	0.18
NECT32	111.92	43.66	1005	Desert steppe	0.20	8	0.17
NECT33	111.89	43.65	1017	Desert steppe	0.26	7	0.17

10 m^2 quadrat for the tree layer, five for the shrub layer (5 × 5 m^2 each) and five for the herb layer (2 × 2 m^2 each). In the dry steppe and desert steppe vegetation in the middle to the west of the transect, we investigated five quadrats in each of the 25 sites. The quadrat size was 1 × 1 m^2 for grasses and 4 × 4 m^2 for shrubs. We created a checklist of vascular species present at each site, and sampled the common species.

Foliage sampling and analysis

Sunlit leaves were obtained with long-handled twig shears. At least 10 g of leaves was collected for each species, except for a small number of species with very small leaves at the dry end of the transect. The samples were subdivided for the measurement of SLA and leaf dry matter content (LDMC) (sample sizes for replicate measurements varied between 0.02 and 2.3 g), C content, N content and δ^{13}C. The measurements used here are the average of three replicates, except in the case of the δ^{13}C where one measurement was made per individual. Leaves were scanned with a laser scanner and the leaf areas were measured using Photoshop on the scanned images. Leaf weight was measured in the field; dry weight was obtained after air-drying for several days and then oven-drying at 75°C for 48 h. Leaf C content was measured by the potassium dichromate volumetry method. N content was measured by the micro-Kjeldahl method. δ^{13}C was measured using a Finnigan MAT DELTAplusXP Isotope Ratio Mass Spectrometer (Finnigan Corporation, San Jose, CA).

Statistical analysis

Principal components analysis (PCA) of climate variables was performed using the SPSS statistical package (SPSS, Chicago, IL, USA). Redundancy analysis (RDA; ter Braak & Prentice, 1988) of traits (as predictands) with respect to climate variables (as predictors) was performed using the program CANOCO (ter Braak & Smilauer, 2002). The traits entered in the analysis were log$_e$ LDMC, log$_e$ C, log$_e$ N, log$_e$ SLA and δ^{13}C. The use of log$_e$-transformed variables allows the directions of various ratios to be inferred from a vector plot (for example, as N$_{area}$ = N/SLA, the vector for log$_e$ N$_{area}$ is the resultant of the vector for log$_e$ N and the vector pointing in the opposite direction to the one for log$_e$ SLA). We used ordinary least-squares regression throughout. Tests for homogeneity of regressions were performed with the SMATR package (Falster et al., 2006).

Results

Variation in climate variables and leaf traits

PCA of climate variables across sampling sites confirmed that there was a single dominant climatic gradient (Table 2)

Table 2 Principal components analysis (PCA) of climate variables, showing strong correlations between all of the moisture-related indices (axis 1), and similarly strong correlations between the temperature-related indices (axis 2)

	Component 1	Component 2
Component matrix		
MAT	0.290	0.921
MAP	0.985	0.051
PJJA	0.947	0.081
mGDD$_0$	−0.336	0.906
MI	0.993	−0.067
mPAR$_0$	−0.861	−0.078
Alpha	0.993	−0.092
Eigenvalues		
% of variance	68.2	24.2
Cumulative %	92.5	

MAP, mean annual precipitation; MAT, mean annual temperature; mGDD$_0$, daily mean during the growing season of accumulated growing degree days above 0°C; MI, moisture index; mPAR$_0$, the daily mean during the growing season of photosynthetically active radiation; PJJA, mean precipitation in June, July and August.

accounting for 68% of the variance. From the wet to the dry end, this gradient was characterized by decreasing MAP, MI, PJJA and alpha, and increasing mPAR$_0$ (attributable to an increasing fraction of hours without clouds). However, a second axis with a nontrivial eigenvalue, accounting for 24% of the variance, was also present, indicating the existence of temperature (MAT and mGGD$_0$) variations independent of the main moisture gradient.

RDA of traits of C$_3$ plants vs the same set of climate variables again showed a single dominant axis reflecting the moisture gradient (Table 3, Fig. 2). The C content of dry weight was almost invariant. Along the gradient from wet to dry, δ^{13}C, LDMC and N$_{area}$ increased while SLA decreased. However, in contrast to the PCA of climate variables alone, the eigenvalue of the second axis was vanishingly small and contributed nothing to the information explained by the climate variables – in other words, although there was some independent variation of climate along a temperature axis, there was no significant associated variation in leaf traits. The sampled variation along the gradient

Table 3 Redundancy analysis of C$_3$ species traits in relation to climate variables

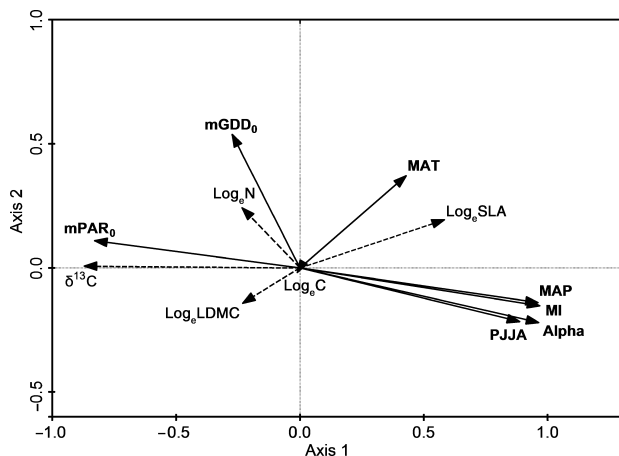|	Axis			
	1	2	3	4
Eigenvalue	0.701	0.003	0.001	0
Trait–environment correlation	0.872	0.346	0.176	0.133
Cumulative % variance of trait data	70.1	70.4	70.5	70.5
Cumulative % variance of trait–environment relations	99.4	99.8	99.9	100

Fig. 2 Redundancy analysis plot showing vectors (representing correlations with the first two axes) for traits and climate variables: $\delta^{13}C$, carbon isotope ratio; $\log_e$ LDMC, $\log_e$ leaf dry matter content; $\log_e$ C, see Q21; $\log_e$ N, see Q21; PJJA, mean precipitation in June, July and August; alpha; MI, moisture index; MAP, mean annual precipitation; $\log_e$ SLA, $\log_e$ specific leaf area; MAT, mean annual temperature; $mGDD_0$, daily mean during the growing season of accumulated growing degree days above $0°C$; $mPAR_0$, the daily mean during the growing season of photosynthetically active radiation.

can thus be taken to reflect control of leaf traits by aridity (with a possible contribution from the associated variation in photosynthetically active radiation), with minimal confounding by temperature.

Variation in $\delta^{13}C$ along the moisture gradient

C_3 plants showed a systematic trend of increasing $\delta^{13}C$ with dryness (Fig. 3), regardless of whether moisture availability was plotted as MAP, MI or alpha. By a small margin, the best R^2 (0.712) was provided by MI, which was used in all subsequent analyses. In a multiple regression of C_3 plant $\delta^{13}C$ with MI, $mGDD_0$ and $mPAR_0$ as predictors (Supporting Information Table S1) only MI had a significant regression coefficient, indicating that temperature and light made no significant additional contributions to explaining the variation in $\delta^{13}C$.

We used linear regressions throughout for simplicity of statistical analysis. However, all three plots showed a tendency for $\delta^{13}C$ to flatten off at the dry end of the transect. C_4 plants showed characteristically higher values of $\delta^{13}C$, and a slight (nonsignificant) trend of decreasing $\delta^{13}C$ with dryness.

Responses of $\delta^{13}C$ for different life forms

The responses of $\delta^{13}C$ to MI for different C_3 life forms (Fig. 4) showed individually significant relationships in all cases but one (lianas/climbers). (None of the C_4 life forms had a significant slope; see Table S2.) There were also small but significant differences (Table S2) between the fitted
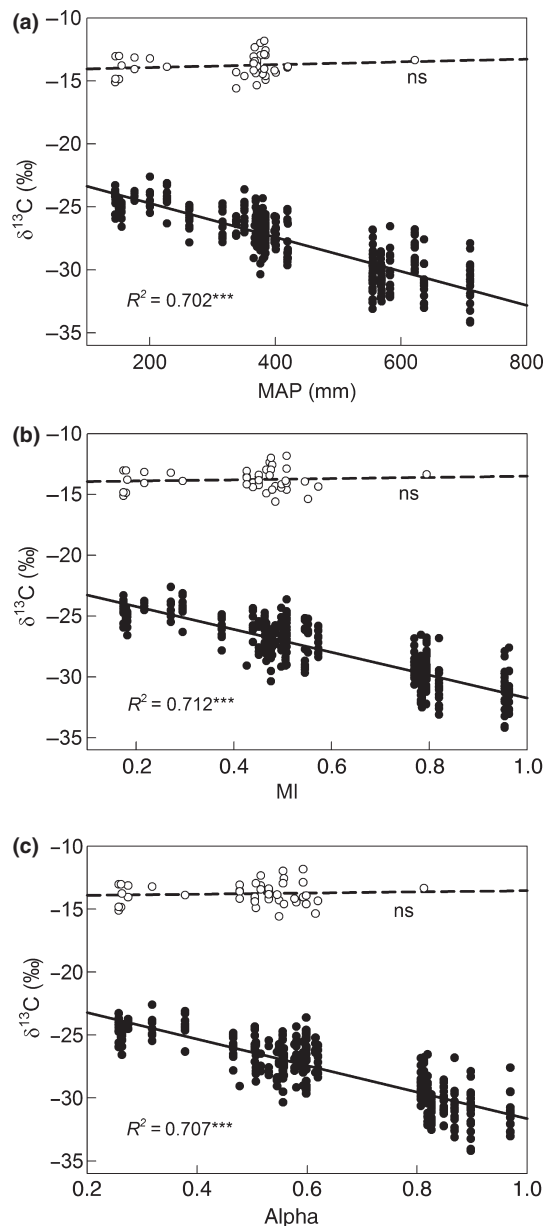

Fig. 3 Relationships between the carbon isotope ratio ($\delta^{13}C$) and three measures of water availability: mean annual precipitation (MAP), moisture index (MI), and alpha. Species are grouped by photosynthetic pathway (C_3 species, closed circles and solid line; C_4 species, open circles and dashed line). ns, not significant. Asterisks indicate the significance levels.

linear regressions for individual life forms and the regression for all C_3 plants (Figs 1, 4). Woody C_3 plants collectively, and trees, had shallower slopes. Nonwoody C_3 plants collectively, and perennial forbs, had steeper slopes, but perennial grasses had a shallower slope. A comparison of average $\delta^{13}C$ values for each life form within three MI 'bins' corresponding to the dry, middle and wet parts of the transect (Table 4) suggested that these differences arose from slight deviations from linearity in the response of different
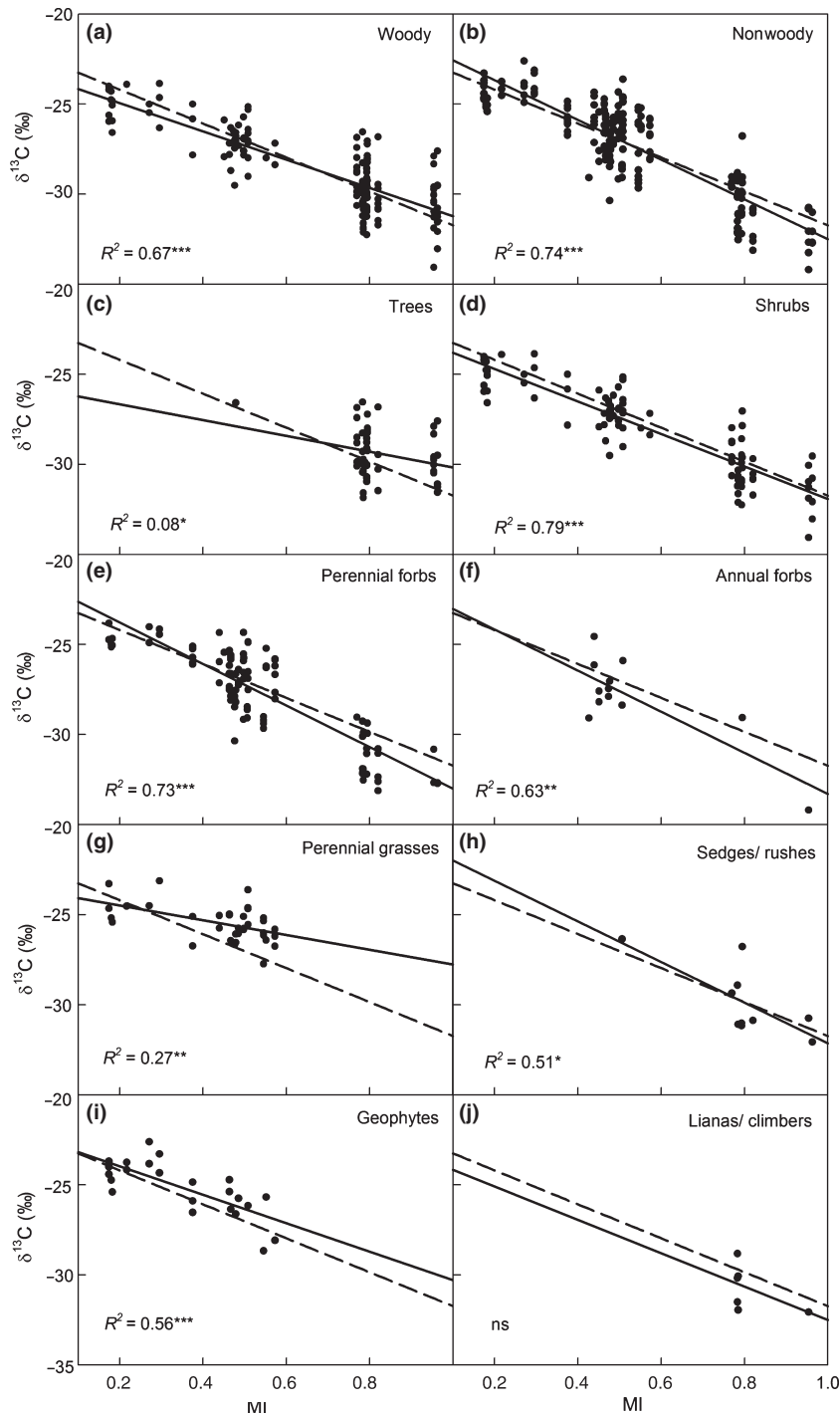
Fig. 4 Relationship between carbon isotope ratio ($\delta^{13}C$) and moisture index (MI) for woody and nonwoody C_3 species, and for C_3 life forms (linear fit, solid line). The linear fit for all C_3 species is shown as a dashed line on all of the panels. ns, not significant. Asterisks indicate the significance levels.

life forms to MI. At the dry end of the transect, there were only very small differences in $\delta^{13}C$ between life forms. In the middle part of the transect, perennial grasses showed significantly higher $\delta^{13}C$ values than shrubs and forbs. At the wet end of the transect, there were systematic and significant differences between life forms, with highest $\delta^{13}C$ values shown by trees, intermediate values by shrubs, and low values by forbs. Subcanopy and especially field-layer

species in forests experience lower D than canopy trees, so this divergence is consistent with a common response to atmospheric dryness.

Responses of other leaf traits

There was a weak tendency for LDMC of C_3 species to increase with dryness, as has been observed previously

Table 4 Multiple comparisons of carbon isotope ratio ($\delta^{13}C$) values for C_3 plant life forms grouped into three bins (moisture index (MI) < 0.35, 0.35–0.7 and > 0.7)

Group	Multiple comparisons when MI ≤ 0.35	Multiple comparisons when 0.35 < MI ≤ 0.7	Multiple comparisons when MI > 0.7
C_3 tree			−29.47 ± 1.34f
C_3 shrub	−24.98 ± 0.87a	−27.09 ± 1.02c	−30.47 ± 1.40gi
C_3 perennial forb	−24.80 ± 0.46ab	−26.91 ± 1.41ce	−31.36 ± 1.27h
C_3 annual forb		−27.23 ± 1.35ce	−31.63 ± 3.63ghi
C_3 perennial grasses	−24.39 ± 0.87ab	−25.75 ± 0.84d	
C_3 sedges/rushes			−30.23 ± 1.61fgi
C_3 lianas/climbers			−30.76 ± 1.29gh
C_3 geophytes	−24.02 ± 0.74b	−26.23 ± 1.17de	

Values are mean ± standard deviation.
Shaded cells indicate that no comparison is possible because the life form is not represented in this part of the transect. Groups sharing a letter do not differ significantly.
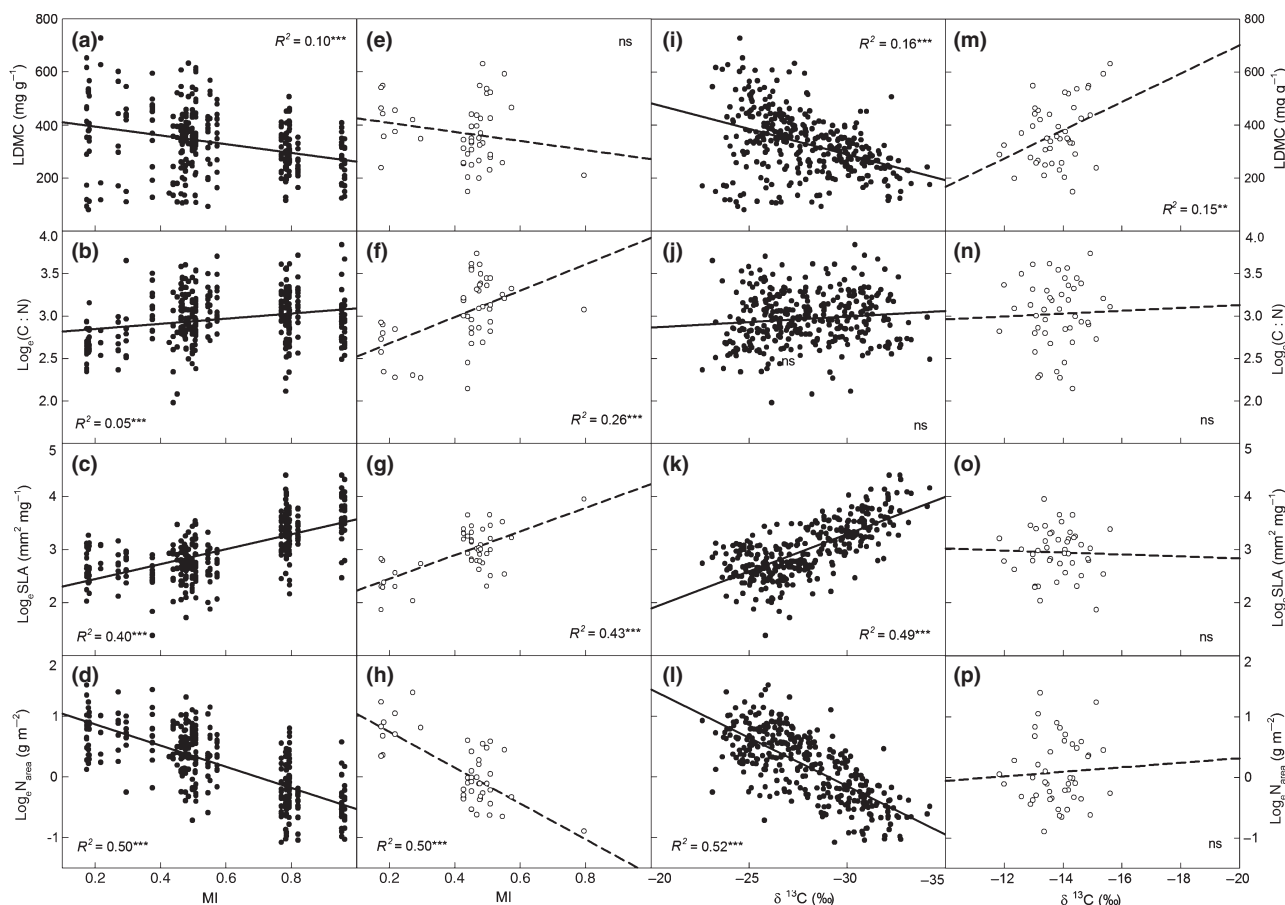

Fig. 5 Relationships between leaf dry matter content (LDMC), $\log_e$ (C : N), $\log_e$ specific leaf area (SLA) and $\log_e$ N per unit leaf area (N_{area}) and carbon isotope ratio ($\delta^{13}C$) for C_3 species (a–d) and C_4 species (e–h), and moisture index (MI) for C_3 species (i–l) and C_4 species (m–p). C_3 species, closed circles and solid line; C_4 species, open circles and dashed line. ns, not significant. Asterisks indicate the significance levels.

(Niinemets, 2001; Lavorel *et al.*, 2007), and a very weak tendency towards narrower C : N ratios (more N per unit C), although this relationship was steeper for C_4 species (Fig. 5). Similarly weak relationships were found for these traits with $\delta^{13}C$ in C_3 plants. By contrast, the data showed a strong increase in N_{area} and decrease in SLA with dryness among both C_3 plants and C_4 plants, and even stronger

relationships of N_{area} and SLA to $\delta^{13}C$ in C_3 plants (Fig. 5). These relationships are highly conserved among life forms and even between C_4 and C_3 plants (Figs 6, 7). The putative relationship of SLA and N_{area} to $c_i : c_a$ cannot be tested for C_4 plants, however, because of the more complex interpretation of $\delta^{13}C$ in C_4 plants (Farquhar, 1983). In multiple regressions of $\log_e N_{area}$ with MI and $\delta^{13}C$ as
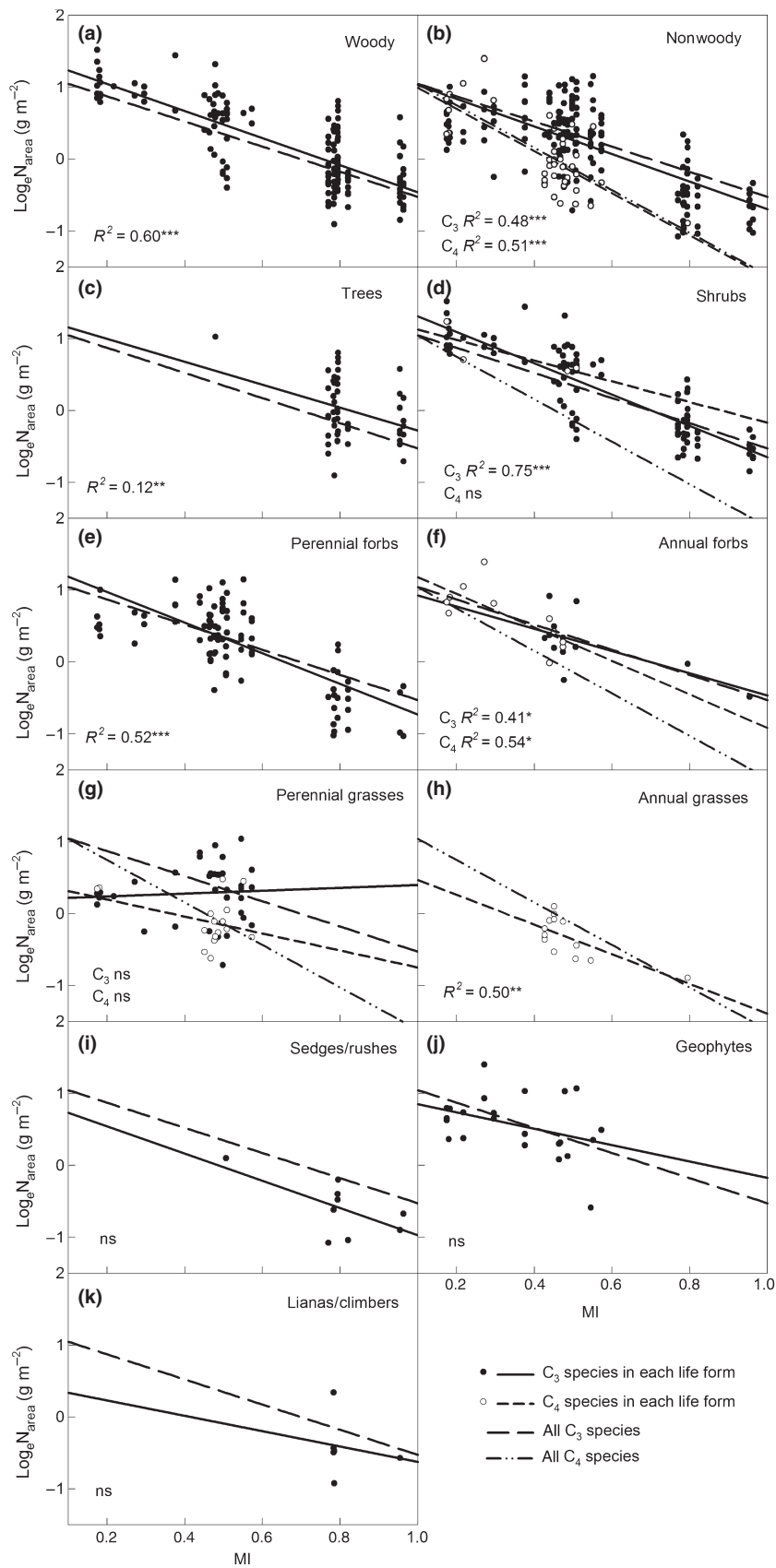
Fig. 6 Relationship between ($\log_e N_{area}$) and moisture index (MI) for C_3 and C_4 woody and nonwoody species, and for C_3 life forms. ns, not significant. Asterisks indicate the significance levels.
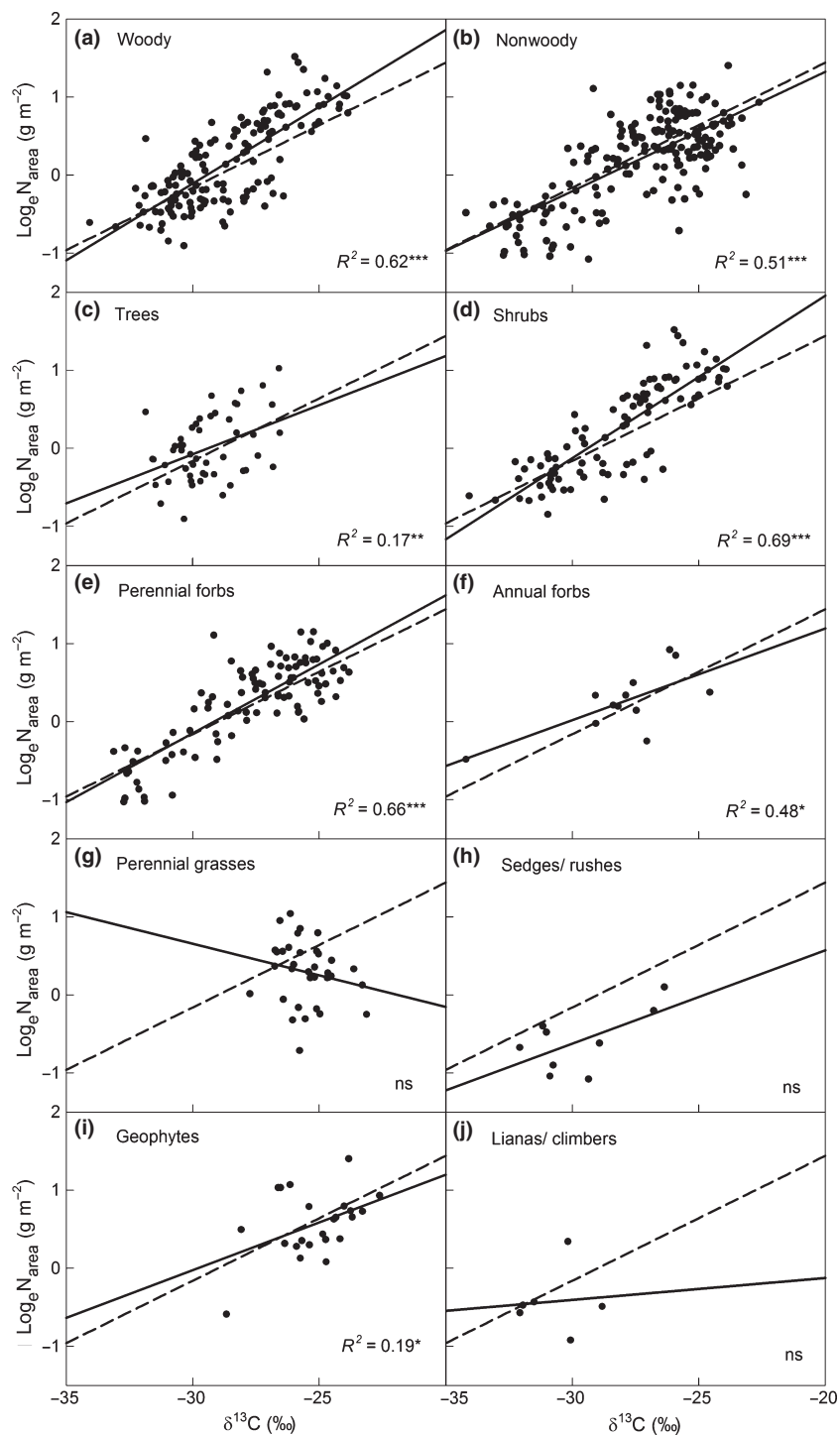
Fig. 7 Relationship between $\log_e$ N per unit leaf area (N_{area}) and carbon isotope ratio ($\delta^{13}C$) for C_3 woody and nonwoody species, and for C_3 life forms (linear fit, solid line). The linear fit for all C_3 species is shown as a dashed line on all of the panels. ns, not significant. Asterisks indicate the significance levels.

predictors (Table S1), C_3 plants showed a significant effect of $\delta^{13}C$ on N_{area}, additional to that of MI.

Responses of $\delta^{13}C$ for different species

Fig. 8 illustrates the responses of $\delta^{13}C$ to MI found within species of C_3 plants, for the 15 C_3 species that were sampled

at five or more sites. The individual species' lines generally did not depart from the overall trend. There was no systematic pattern of offsets and, in particular, there was no indication that species of drier environments compensate by having lower $\delta^{13}C$ at a given MI, as hypothesized by Schulze *et al.* (1998, 2006). Instead, species tended to be replaced (in the direction of increasing dryness) by species
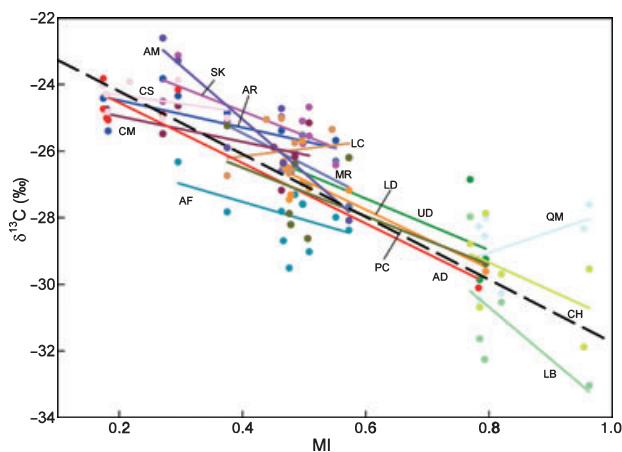
Fig. 8 Relationship between carbon isotope ratio (δ^{13}C) and moisture index (MI) for all C_3 species that were sampled at five or more sites. AD, *Asparagus dauricus*; AF, *Artemisia frigida*; AM, *Allium mongolicum*; AR, *Allium ramosum*; CH, *Corylus heterophylla*; CM, *Caragana microphylla*; CS, *Caragana stenophylla*; LB, *Lespedeza bicolour*; LD, *Lespedeza davurica*; LC, *Leymus chinensis*; MR, *Melitoides ruthenica*; PC, *Potentilla chinensis*; QM, *Quercus mongolica*; SK, *Stipa krylovii*; UD, *Ulmus davidiana* var. *japonica*.

that had higher δ^{13}C, but the same δ^{13}C at a given MI. The only species with an individually significant regression that differed significantly from the general line was the geophyte of dry environments *Allium racemosum*, whose slope against MI was shallower than the norm, consistent with the general flattening of the multi-species δ^{13}C–MI relationship at low MI. Species at the wet end of the transect also showed a (nonsignificant) tendency to diverge in their δ^{13}C–MI relationship; for example, the tree species *Quercus mongolica* showed higher δ^{13}C values than the shrub species *Lespedeza bicolor*. We also examined the responses of δ^{13}C to MI for three C_4 species (*Cleistogenes squarrosa*, *Pennisetum flaccidum* and *Salsola collina*): none showed significant slopes (Table S2).

Discussion

These findings, obtained under optimum field sampling conditions on a long precipitation gradient (130–900 mm) with minimal confounding by temperature or latitude, provide evidence for close to universal scaling (i.e. the same response both within and between C_3 species and life forms) of δ^{13}C. C_3 species that successively replaced one another as the environment became drier fell along a single overall trend of δ^{13}C in relation to MI. They did not have lower δ^{13}C at the same MI, as one would expect according to the biotic homoeostasis hypothesis proposed by Schulze *et al.* (1998, 2006). Thus, in common with Wittmer *et al.* (2008), our results show that species- and community-level responses to changing aridity are strikingly similar. Given the lack of any compelling evidence presented to date in favour of the biotic

homoeostasis hypothesis, and its clear rejection by our results, we suggest that it should be abandoned.

The results have valuable implications for large-scale modelling. They support the simplifying assumption that different C_3 species and life forms react through stomatal adjustment in a similar way in response to the aridity gradient. This is consistent with the theoretical expectation that the plants are responding to a common atmospheric property (D). However, the magnitude of the variation in δ^{13}C along the gradient was too large to be plausibly accounted for by the response of $c_i : c_a$ to D with constant ξ (B. Medlyn, pers. comm.). The results therefore imply a systematic adjustment of the ξ parameter along the gradient. They further indicate that (within the sampled range of MAP) this adjustment is universal, following the same pattern within as between species. Differences among life forms were slight, and could reasonably be neglected for modelling purposes.

The fact that the relationships of N_{area} and SLA in C_3 plants were stronger with δ^{13}C than MI suggests that there is a systematic relationship that applies to a part of the variation within sites at the same MI – in other words, that there is a mechanistic link among the leaf traits such that low $c_i : c_a$ ratios tend to be accompanied by low SLA and high N_{area}, and that this may account at least in part for the observed relationships of SLA and N_{area} to MI. The observed relationships to δ^{13}C in C_3 plants are qualitatively consistent with the hypothesis (e.g. Wright *et al.*, 2003) that high photosynthetic capacity coupled with high CO_2 drawdown represents an adaptation to drought. Low $c_i : c_a$ ratios, adaptive under water-stressed conditions, imply that leaves require a high N_{area} in order to achieve the high carboxylation capacity required to effectively utilize the available light when c_i is low. This mechanism may be further strengthened because PAR increases with decreasing cloudiness, so more light is available to be utilized towards the dry end of the gradient. Low SLA can be viewed as a requirement for leaves to be capable of high potential carboxylation rates.

However, the magnitude of the increase in N_{area} (by a factor of 4.5) along the gradient was considerably larger than would be indicated by the hypothesis that carboxylation capacity at the leaf level adapts to the environment in such a way as to achieve maximal net photosynthesis, that is, around the point of co-limitation by Rubisco and PAR (Farquhar *et al.*, 1982; Haxeltine & Prentice, 1996). This hypothesis would predict an increase by a factor of only 1.6 in the carboxylation capacity of C_3 plant leaves as a result of the combination of increasing $mPAR_0$ (by a factor of 1.25 along the transect) and decreasing $c_i : c_a$. Thus, the magnitude of the changes in N_{area} and SLA along the transect requires an additional functional explanation. Furthermore, any comprehensive explanation for these observations must apply to C_4 as well as C_3 plants: the response of N_{area} and SLA to MI in C_4 plants contrasts sharply with their lack of response in δ^{13}C. The low SLA and high N_{area} of plants towards the

dry end of the gradient may be functionally related to the greater resistance to dehydration conferred by stiffer leaves (Niinemets, 2001; Harrison *et al.*, 2010), or to the requirement for leaves to be small or narrow to avoid overheating under conditions of high radiation load and low transpiration rates (Midgley *et al.*, 2004; Harrison *et al.*, 2010).

The plant species sampled were almost all angiosperms. There is some evidence that the $c_i : c_a$ ratio (Lloyd & Farquhar, 1994) and $\delta^{13}C$ (Marshall & Waring, 1984) of gymnosperms react more steeply to increasing D, although one study of the $\delta^{13}C$ of respired CO_2 from temperate angiosperm- and gymnosperm-dominated forests in the same climate indicated no difference in the response to D (Mortazavi *et al.*, 2005). The possible difference could be tested by sampling along a comparable moisture gradient in a temperate winter rainfall regime where conifers dominate. The gymnosperms sampled on the NECT (*Pinus koraensis*, *Pinus tabulaeformis* and *Larix olgensis*) did not have atypical $\delta^{13}C$ values for their position along the transect. However, no gymnosperm species were encountered in the middle or dry sections of the transect.

Our sampling stopped at a MAP of 130 mm, so we did not sample vegetation in hyper-arid environments. There is an indication in the overall data (Fig. 3) and in the data for one species (*Allium racemosum*; Fig. 8) that the general response of leaf $\delta^{13}C$ to MI levelled off at MI values below 0.3. The values of $\delta^{13}C$ reached at this low level of MI may be approaching minimum sustainable values of $c_i : c_a$. Taking $\delta^{13}C$ in atmospheric CO_2 as $-8.3‰$ (Mauna Loa, July 2006: http://scrippsco2.ucsd.edu/data/atmospheric_co2.html) and applying standard approximations $\Delta \approx \delta_{air} - \delta_{leaf} \approx a + (b - a)\, c_i : c_a$, $a = 4.4$ and $b = 27$, a leaf $\delta^{13}C$ of $-24‰$ would correspond to a $c_i : c_a$ ratio of 0.5. Lower average $c_i : c_a$ ratios may not allow sufficient carbon assimilation for plant survival. Vegetation in the driest environments may therefore depend strictly on access to groundwater to allow increased transpiration rates. This could be an explanation for the extremely variable results obtained by Schulze *et al.* (2006) for *Eucalyptus* spp. at low MAP. Dependence of vegetation on aquifers was also invoked by Schulze *et al.* (1996) to explain the atypical constancy of $\delta^{13}C$ values of C_3 foliage along a precipitation gradient eastward from the Andes mountains. A different modelling approach may be required to describe vegetation subsisting under hyperarid conditions, and perhaps also in situations where groundwater is the dominant water source. The indication in our data that the $\delta^{13}C$ values of C_3 plant leaves at the dry end of the NECT are approaching a maximum could be tested by a westward extension of the transect.

Acknowledgements

References

Bowling D, McDowell N, Bond B, Law B, Ehleringer J. 2002. ^{13}C content of ecosystem respiration is linked to precipitation and vapor pressure deficit. *Oecologia* **131**: 113–124.

ter Braak CJF, Prentice IC. 1988. A theory of gradient analysis. *Advances in Ecological Research* **18**: 271–317.

ter Braak CJF, Smilauer P. 2002. *CANOCO reference manual and user's guide to Canoco for Windows: software for canonical community ordination (version 4.53).* Ithaca, NY, USA: Microcomputer power.

Cowan IR, Farquhar GD. 1977. Stomatal function in relation to leaf metabolism and environment. *Society Experimental Biology Symposium* **31**: 471–505.

Diefendorf AF, Mueller KE, Wing SL, Koch PL, Freeman KH. 2010. Global patterns in leaf ^{13}C discrimination and implications for studies of past and future climate. *Proceedings of the National Academy of Sciences, USA* **107**: 5738–5743.

Falster DS, Warton DI, Wright IJ. 2006. SMATR: Standardised major axis tests and routines, ver 2.0 [WWW document]. URL http://www.bio.mq.edu.au/ecology/SMATR/. Last accessed: 1 August 2010.

Farquhar GD. 1983. On the nature of carbon isotope discrimination in C_4 species. *Australian Journal of Plant Physiology* **10**: 205–226.

Farquhar GD, O'Leary MH, Berry JA. 1982. On the relationship between carbon isotope discrimination and the intercellular carbon dioxide concentration in leaves. *Australian Journal of Plant Physiology* **9**: 121–137.

Farr TG, Rosen PA, Caro E, Crippen R, Duren R, Hensley S, Kobrick M, Paller M, Rodriguez E, Roth L et al. 2007. The shuttle radar topography mission. *Reviews of Geophysics* **45**: RG2004. doi:10.1029/2005RG000183.

Gallego-Sala AV, Clark JM, House JI, Orr HG, Prentice IC, Smith P, Farewell T, Chapman SJ. 2010. Bioclimatic envelope model of climate change impacts on blanket peatland distribution in Great Britain. *Climate Research*, doi:10.3354/cr00911.

Harrison SP, Prentice IC, Barboni D, Kohfeld KE, Ni J, Sutra J-P. 2010. Ecophysiological and bioclimatic foundations for a global plant functional classification. *Journal of Vegetation Science* **21**: 300–317.

Haxeltine A, Prentice IC. 1996. A general model for the light use efficiency of primary production. *Functional Ecology* **10**: 551–561.

Hutchinson M, Hancock PA. 2006. Spatial interpolation of large climate data sets using bivariate thin plate smoothing splines. *Environmental Modelling and Software* **21**: 1684–1694.

Katul G, Manzoni S, Palmroth S, Oren R. 2010. A stomatal optimization theory to describe the effects of atmospheric CO_2 on leaf photosynthesis and transpiration. *Annals of Botany* **105**: 431–442.

Lavorel S, Díaz S, Cornelissen JHC, Garnier E, Harrison SP, McIntyre S, Pausas JG, Perez-Harguindeguy N, Roumet C, Urcelay C et al. 2007. Plant functional types: are we getting any closer to the Holy Grail? In: Canadell JG, Pataki D, Pitelka L, eds. *Terrestrial ecosystems in a changing world. The IGBP Series.* Berlin, Heidelberg, Germany: Springer-Verlag, 149–160.

Liu W, Xiahong F, Youfeng N, Qingle Z, Yunning C, Zhisheng AN. 2005. $\delta^{13}C$ variation of C_3 and C_4 plants across an Asian monsoon

rainfall gradient in arid northwestern China. *Global Change Biology* 11: 1094–1100.

Lloyd JJ, Farquhar GD. 1994. ^{13}C discrimination during CO_2 assimilation by the terrestrial biosphere. *Oecologia* 99: 201–215.

Marshall JD, Waring RH. 1984. Conifers and broadleaf species: stomatal sensitivity differs in western Oregon. *Canadian Journal of Forest Research* 14: 905–908.

Midgley GF, Aranibar JN, Mantlana KB, Macko S. 2004. Photosynthetic and gas exchange characteristics of dominant woody plants on a moisture gradient in an African savanna. *Global Change Biology* 10: 309–317.

Miller JM, Williams RJ, Farquhar GD. 2001. Carbon isotope discrimination by a sequence of *Eucalyptus* species along a subcontinental rainfall gradient in Australia. *Functional Ecology* 15: 222–232.

Monteith JL. 1995. Accomodation by transpiring vegetation and the convective boundary layer. *Journal of Hydrology* 166: 251–263.

Mortazavi B, Chanton JP, Prater JL, Oishi C, Oren R, Katul GG. 2005. Temporal variability in ^{13}C of respired CO_2 in a pine and a hardwood forest subject to similar climatic conditions. *Oecologia* 142: 57–69.

Mott KA, Parkhurst DF. 1991. Stomatal responses to humidity in air and helox. *Plant, Cell & Environment* 14: 509–515.

Ni J, Wang GH. 2004. Northeast China Transect (NECT): ten-year synthesis and future challenges. *Acta Botanica Sinica* 46: 379–391.

Ni J, Zhang X-S. 2000. Climate variability, ecological gradient and the Northeast China Transect (NECT). *Journal of Arid Environments* 46: 313–325.

Niinemets N. 2001. Global-scale climatic controls of leaf dry mass per area, density, and thickness in trees and shrubs. *Ecology* 82: 453–469.

Palmroth S, Berninger F, Nikinmaa E, Lloyd J, Pulkkinen P, Hari P. 1999. Structural adaptation rather than water conservation was observed in Scots pine over a range of wet to dry climates. *Oecologia* 121: 302–309.

Pieruschka R, Huber G, Berry JA. 2010. Control of transpiration by radiation. *Proceedings of the National Academy of Sciences, USA* 107: 13372–13377.

Prentice IC, Sykes MT, Cramer W. 1993. A simulation model for the transient effects of climate change on forest landscapes. *Ecological Modelling* 65: 51–70.

Saxton KE, Rawls WJ. 2006. Soil water characteristic estimates by texture and organic matter for hydrologic solutions. *Journal of the Soil Science Society of America* 70: 1569–1578.

Schulze E-D, Mooney HA, Sala OE, Jobbagy E, Buchmann N, Bauer G, Canadell J, Jackson RB, Loreti J, Oesterheld M. 1996. Rooting depth, water availability, and vegetation cover along an aridity gradient in Patagonia. *Oecologia* 108: 503–511.

Schulze E-D, Turner NC, Nicolle D, Schumacher J. 2006. Leaf and wood carbon isotope ratios, specific leaf areas and wood growth of *Eucalyptus*

species across a rainfall gradient in Australia. *Tree Physiology* 26: 479–492.

Schulze ED, Williams RJ, Farquhar GD, Schulze W, Langridge J, Miller JM, Walker BH. 1998. Carbon and nitrogen isotope discrimination and nitrogen nutrition of trees along a rainfall gradient in northern Australia. *Australian Journal of Plant Physiology* 25: 413–425.

Shi XZ, Yu DS, Warner ED, Pan XZ, Petersen GW, Gong ZG, Weindorf DC. 2004. Soil database of 1:1,000,000 digital soil survey and reference system of the Chinese genetic soil classification system. *Soil Survey Horizons* 45: 129–136.

Stewart GR, Turnbull MH, Schmidt S, Erskine PD. 1995. ^{13}C natural abundance in plant communities along a rainfall gradient: a biological integrator of water availability. *Australian Journal of Plant Physiology* 22: 51–55.

Wang GH, Ni J. 2005. Responses of plant functional types to an environmental gradient on the Northeast China Transect. *Ecological Research* 20: 563–572.

Wittmer MHOM, Auerswald K, Tungalag R, Bai YF, Schäufele R, Schnyder H. 2008. Carbon isotope discrimination of C3 vegetation in Central Asian grassland as related to long-term and short-term precipitation patterns. *Biogeosciences* 5: 913–924.

Wright IJ, Reich PB, Westoby M. 2003. Least-cost input mixtures of water and nitrogen for photosynthesis. *American Naturalist* 161: 98–111.

Supporting Information

Additional supporting information may be found in the online version of this article.

Table S1 Results from multiple regression analyses

Table S2 Simple regression analyses: relationship, slope, intercept, R^2, *P*-value for slope, and *P*-value for the change from the slope of all C_3 species or all C_4 species (as appropriate)

Please note: Wiley-Blackwell are not responsible for the content or functionality of any supporting information supplied by the authors. Any queries (other than missing material) should be directed to the *New Phytologist* Central Office.